# Applications of acoustic microscopy to petrophysical studies of reservoir rocks

*Manika Prasad, Stanford University*

SUMMARY

Microstructural variations significantly affect seismic wave propagation. Traditional techniques for studying microstructure either give surface information or are limited in resolution. I demonstrate here the use of acoustic microscopy to study microstructural and macrostructural impedance variations in reservoir rocks. Using various frequencies allows us to make qualitative maps of impedance variations in different scales. Quantitative analyses of elastic impedance and 3D volumetric analyses are among the useful applications of this technique to petrophysical studies of reservoir rocks.

INTRODUCTION

Various methods have been employed to characterize microstructural properties of reservoir rocks. The goals of such characterization are to relate microstructure as well as other lithological characteristics to velocity and attenuation properties of these rocks. Traditionally, microscopic imaging techniques such as scanning electron microscopy (SEM), transmission electron microscopy (TEM), and optical microscopy have been used to study the grains, cementation, and pore structures of rocks (Winkler, 1983; Murphy et al., 1984; Christensen and Wang, 1985; O'Brien et al., 1992). Here, I show applications of a recently developed technique, scanning acoustic microscopy, to study the microstructure of reservoir rocks and its effects on the elastic and anelastic properties.

The principle of acoustic microscopy (AM) is to scan the acoustic properties (impedance, $\rho \cdot V$, where $\rho$ = density, V = acoustic velocity) of a sample and to provide an image of the microstructural features on the basis of impedance contrasts in the grains and between the various interfaces in the sample. Thus, in addition to grain shape, grain cementation and contact, and pore space characterization, grain clusters with comparable impedance can be identified. Acoustic waves can propagate through optically opaque materials which makes acoustic microscopy an important non-destructive tool to study micro- and macrostructural properties of rocks.

Few studies have reported results of acoustic microscopy on rock samples (Rodriguez-Rey et al., 1990; Briggs, 1992; Prasad and Manghnani, 1996; 1997). For example, it has been used for identifying microcracks in quartz grains in granites (Ilett et al., 1984), for distinguishing between different mineral phases (Briggs, 1985), to study impedance anisotropy in rocks (Prasad and Manghnani, 1996) and to evaluate interfacial bonds and microstructure in concrete (Prasad et al., 1996). Recent studies have shown that considering grain size alone does not explain scattering effects observed in ultrasonic pulse transmission experiments (Blair, 1990; Lucet and Zinszner, 1992), and that clusters of grains with comparable impedance act as scatterers for ultrasonic waves.

METHOD

A scanning acoustic microscope consists of three main units:

1. The Acoustic and Scanning Unit consists of a transducer to generate and register acoustic waves, a sapphire rod which acts as a wave guide and a sample stage which is movable in X, Y, and Z directions.

   A ZnO transducer sputtered on one end of a sapphire rod generates high frequency acoustic waves. The sapphire rod functions as a channel for the acoustic waves. A cavity at the bottom of the sapphire rod focuses the waves through a coupling fluid (distilled water) at a specific position on the sample. Reflected waves from the specimen return through the sapphire rod to the transducer, where they are converted into electrical signals. Together, the transducer and the sapphire rod are referred to as the acoustic lens.

2. The Pulse Generator and Receiver Unit consists of a high frequency pulse generator that emits short pulses to excite the transducer and a receiver to amplify and record the reflected signals registered by the transducer. An r.f. (radio frequency) switching device allows separation between transmitted and received signals.

3. The Image Storage, Display and Control Unit is a 586/133 Mhz computer system with scanning and image control plug-in cards. It allows control over stage manipulation in X, Y and Z directions. The image control transforms the electrical signals from the transducer into a gray or color scaled image with 5 12

pixels in X and Y directions with 256 shades of gray or color (8 bit).

The lens is scanned in a raster pattern over the specimen in order to form an image. Results of AM of shales and sandstones using two scanning acoustic microscopes, a high frequency (0.06 -- 2 GHz) acoustic microscope (Ernst Leitz scanning acoustic microscope, ELSAM, now marketed by Krämer Scientific Instruments) and a low frequency (25 -- 100 MHz) acoustic microscope (SAM50) will be presented. Both microscopes operate in reflection mode. The depth of penetration and resolution of microstructural features depend on the operating frequency. Acoustic lenses of different frequencies are used to examine the samples: High frequency (1.2 and 0.2 GHz) lenses are used in the ELSAM system for high resolution scanning of up to 1 mm2 area (about 1 µm at 1.2 GHz). 25 MHz lens is used in the SAM system to larger scan (20 mm x 20 mm) with resolution of about 60 µm and penetration depths of 6 - 8 mm.

In the low frequency AM system, the microstructure is mapped by longitudinal wave propagation and by studying the reflections from the top and bottom of objects or layers with different acoustic impedances. In the high frequency ELSAM system, design and curvature of the high frequency acoustic lenses are optimized to achieve a high sensitivity to surface acoustic (Rayleigh) waves. Such a design allows us to map microstructural features from the interference patterns between normally reflected longitudinal waves and the Rayleigh waves.

Figure 1 shows a ray model of an acoustic lens. Two types of waves are observed: longitudinal waves and Rayleigh waves. Longitudinal waves that are incident at a Rayleigh angle on the sample excite Rayleigh waves. In acoustic imaging of materials with reasonable stiffness, such as rocks, a dominant role is played by these Rayleigh waves that travel slower than longitudinal and shear waves and are confined to within a depth of about a wavelength from the surface (Rodriguez-Rey et al., 1990).

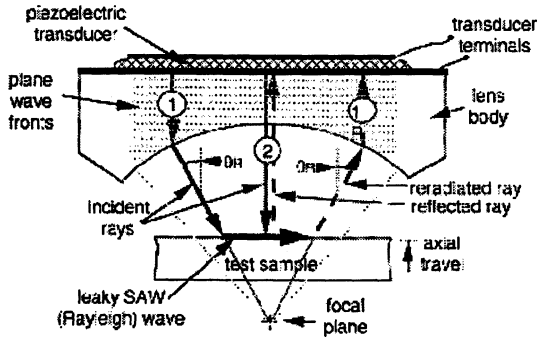


Fig. 1. Schematic diagram of ray paths in acoustic microscopy. Only rays 1 and 2 contribute to the impedance information gathered at the transducer. Rays incident at a Rayleigh angle of $\theta_R$ generate Rayleigh waves (from Weglein, 1996).

These Rayleigh waves continuously leak energy back into the coupling fluid and produce an interference signal with the central part of normally reflected rays. To produce a surface image, the acoustic beam is focused on the sample surface. A "defocused" image is produced by moving the sample towards the acoustic lens such that the focal point of the acoustic beam is below the sample surface (It should be noted here that a 'defocused' image is not out of focus or fuzzy, but that it contains information from both surface and subsurface, with the Rayleigh waves providing the subsurface information.). As the distance between the lens and sample surface is reduced, the signal received by the transducer undergoes a series of changes. The V(z) curve, that is, amplitude of signal received (V) as a function of distance between lens and sample (z) is a material characteristic. It has an oscillating shape due to constructive and destructive interference between the central part of the normally reflected waves and Rayleigh waves. Any change in material properties affects the V(z) curve and with it the color contrast in the image. Rayleigh wave velocity can be determined from the maxima and minima of a V(z) curve. For a comprehensive and rigorous documentation of high frequency acoustic microscopy and V(z) analyses, the reader is referred to Briggs (1992).

## EXAMPLES

Quantitative and qualitative analyses of impedance variations in sandstone and shale samples will be presented. The scale of measurements depends on the operating frequency.

### Qualitative Analyses

In its simplest form, AM can be used to make an X-Y image of surface and sub-surface features. Here, the lens is scanned in X-Y direction at fixed Z position on the sample. The color coded image of the signal received by the transducer gives a map of the impedance variations. Figures 2 and 3 show typical C-scans in two sandstone samples made at 1 GHz. In both images, grains are light gray, alteration effects are darker gray and pore spaces are black colored. Apart from grain and pore space configurations, contact areas can be compared between the two samples. In Figure 2, grains are separated by a wide contact area that has a different impedance from the grains, whereas the sandstone in Figure 3 shows comparable impedance of grains and contacts.

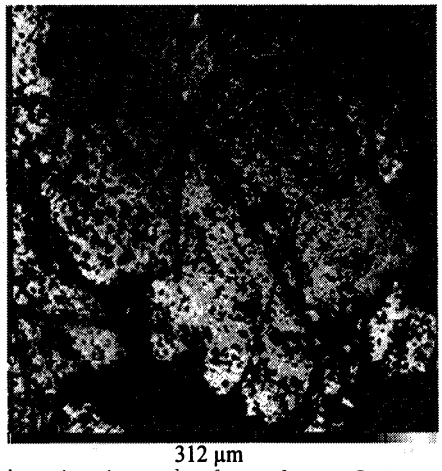


Fig. 2. Acoustic micrograph of a sandstone. Grains are light gray, alteration effects as dark gray and pore spaces are black colored. The image was made at 1 GHz (from Prasacd and Manghiani, 1997).

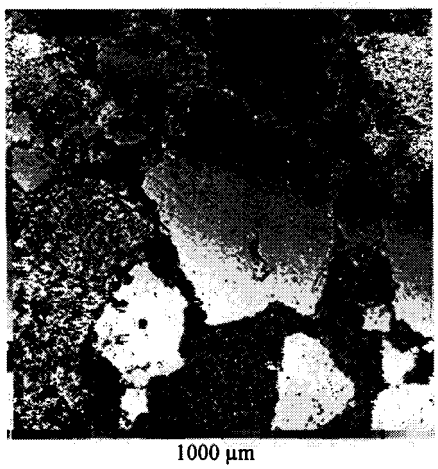


**Fig. 3. Acoustic micrograph of a sandstone. Grains are light gray, alteration effects as dark gray and pore spaces are black colored. The image was made at 1 GHz (from Prasad and Manghnani, 1997).**

Rayleigh Wave Velocity

In C-scan images, material properties (Rayleigh wave velocity, $V_R$) can be quantified from any interference fringes which might be present. Interference fringes, produced at discontinuities such as grain and sub-grain boundaries allow us to estimate VR from their spacing, $\lambda_R$; $V_R = \lambda_R \cdot f$, &frequency (Briggs, 1985). Figure 4 shows an example of a cement mortar sample with Rayleigh fringes in a quartz grain. The prominent dark line in the middle of the image marks a discontuinity. rayleigh fringes are the less prominent lines running parallel to segments of the discontinuity.

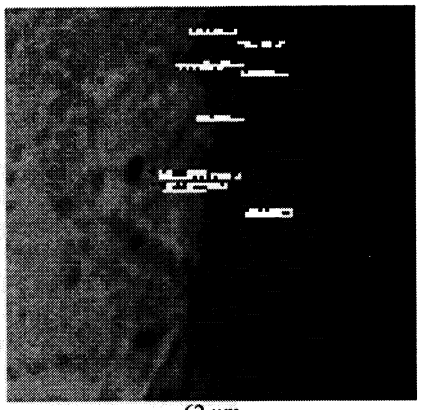


Fig. 4 Acoustic micrograph of a cement mortarsample. Intragranular boundary in a quartz grain shows interference fringes at a spacing of 2.19 µm giving a $V_R$ = 3498 m/s. The image was made at 1 GHz (from Prasad et al., 1996).

3D Volumetric Analyses

Volumetric imaging is possible using low frequency AM. Low frequency acoustic waves can penetrate up to 6-8 mm in the sample. A 3D image of the microstructure can be made by combining multiple B-scans (X-Z scans) made at various locations on the sample. For example, Prasad and Manghnani (1996) have mapped dipping layers of bright and dull coal in a coal sample using this technique.

V(z) analyses

Figure 5 shows effects of V(z) curve on color contrast in an image of a tooth enamel (Briggs, 1992). At focus, the curves overlap and no color contrast is observed in Figure 6a. With increasing defocus, the normally reflected Rayleigh waves alternate in being in and out of focus. Furthermore, due to local variations in material properties, the V(z) curves are separated and so the image gains contrast with defocus. VR can be determined from this V(z) curve (Briggs, 1992).

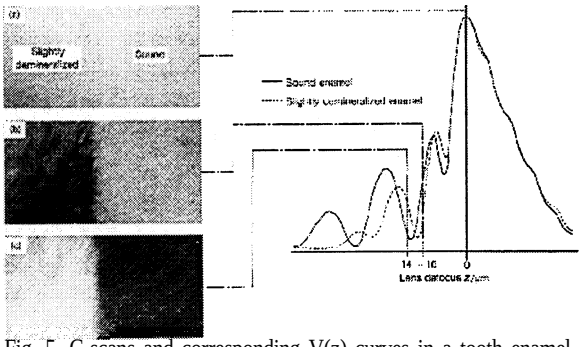


Fig. 5. C-scans and corresponding V(z) curves in a tooth enamel. At z=0, the curves overlap. At z=-10 µm, and z=-14 µm the curves separate, with a reversal at z=-14 µm (from Briggs, 1992).

Acoustic Materials Signature

A further development of V(z) curves has been recently reported (Hirsekom and Pangraz, 1994). This technique utilizes the initial part of a V(z) curve. The so called AMS (Acoustic Materials Signature) is used to determine VR from the distance between the maximum of specular reflection and the first interference maximum. Figure 6 shows a typical AMS in a V(z) curve. Region marked AMS2 contains information about material properties (Hirsekom and Pangraz, 1994; Hirsekom et al., 1995; Weglein, 1996)

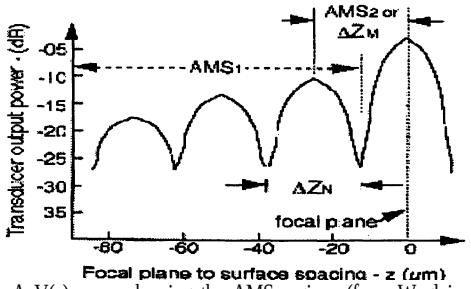


Fig. 6. A V(z) curve showing the AMS regions (from Weglein, 1996).

CONCLUSIONS

AM can be used to make qualitative and quantitative impedance characterizations of reservoir rocks. Main advantage of AM are its non-destructive capability to image surface and sub-surface features based on impedance changes. Quantifying impedance changes will greatlt improve our understanding of seismic wave propagation in reservoir rocks.

ACKNOWLEDGMENTS

Part of this work was done when I was at the University of Hawaii. Many thanks are due to Murli H. Manghnani for discussions and support during my stay at the University of Hawaii. I wish to thank Silvia Pangraz and Walter Arnold of the Fraunhofer (IzfP) Institute in Saarbriicken for discussions, and Kramer Scientific Instruments for support of the instrumental facility.

REFERENCES

Blair, D. P., 1990, A direct comparison between vibrational resonance and pulse transmission data for assessment of seismic attenuation in rocks: Geophysics, 55, 51-60.

Briggs, G. A. D., 1985, An introduction to scanning acoustic microscopy: Royal Microscopical Society Handbook, 12, Oxford University Press, Oxford.

Briggs, G. A. D., 1992, Acoustic Microscopy: Monographs on the Physics and Chemistry of Materials, 47, Oxford Science Publications.

Christensen, N. I., and Wang, H. F., 1985, The influence of pore and confining pressure on dynamic elastic properties of Berea sandstone: Geophysics, 50,207.2 13.

Hirsekorn, S., and Pangraz, S., 1994, Materials characterization with the acoustic microscope: Appl. Phys. Lett., 64, 1632-1634.

Hirsekorn, S., Pangraz, S., Weides, G., Arnold, W., 1995, Measurement of elastic impedance with high spatial resolution using acoustic microscopy: Appl. Phys. Lett., 67,745,747.

Ilett C., Somekh, M. G., and Briggs, G. A. D. 1984, Acoustic microscopy of elastic discontinuities. Proc. R. Soc. Lond., A393, 171-183.

Lucet, N., Zinszner, B., 1992, Effects of heterogeneities and anisotropy on sonic and ultrasonic attenuation in rocks: Geophysics, 57, #8, 10 18-l 026.

Murphy, W. F., Yale, R. O., Winkler, K. W., 1984, Centimeter scale heterogeneities and ministratification in sedimentary rocks: Geophys. Res. Lett., 11, #8,697-700.

O'Brien D. K., Manghnani, M. H., Tribble, J. S., Wenk, H.-R., 1992, Preferred orientation and velocity anisotropy in marine clay-bearing calcareous sediments: in Carbonate Microfabrics, R. Rezak, D. L. Lavoie (eds.), Springer Verlag, 149-161.

Prasad, M., Manghnani, M. H., 1996, Velocity and impedance microstructural anisotropy in reservoir rocks: SEG 66th Annual Internat. Mtg., Soc. Expl. Geophys., Expanded Abstracts, 1854-1857.

Prasad, M., Manghnani, M. H., 1997, Effects of pore and differential pressures on compressional wave velocity and quality factor on Berea and Michigan sandstones: Geophysics, In press.

Prasad, M., Manghnani, M.H., and Livingston, R.A., Scanning acoustic microscopy for evaluating interfacial bonds and microstructure in Portland cement concrete: Proc. 1st US-Japan Symposium on Advances in NDT, Amer Soc. for Nondestructive Testing, OH, 3 74-3 79.

Rodriguez-Rey, A., Briggs, G. A. D., Field, T. A., and Montoto, M., 1990, Acoustic microscopy of rocks: J. Microsc., 160,21-30.

Winkler, K. W., 1983, Contact stiffness in granular porous materials. Comparison between theory and experiments: Geophys. Res. Lett., 10, 1073-1076.

Weglein, R.D., 1996, Extended Acoustic Material Signature: Proc. 1st US-Japan Symposium on Advances in NDT, Amer Soc. for Nondestructive Testing, OH, 193-l 98.